mal phonons by electrons localized at dislocations but this subject has not yet been investigated.

It should be pointed out that the oscillatory effects mentioned above are strongest at sufficiently low temperatures and for regular dislocation structures. Increase in temperature and the concentration broadening of a spectrum of localized electrons, analyzed in Sec. 2, broaden the oscillatory pattern. The estimates obtained in Refs. 17 and 18 show that these effects are fairly minute and attempts to discover them should be accompanied by special measures to produce ordered high-density dislocation structures.

[1] V. L. Bonch-Bruevich and V. B. Glasko, Fiz. Tverd. Tela (Leningrad) **3**, 36 (1961) [Sov. Phys. Solid State **3**, 26 (1961)].
[2] V. L. Bonch-Bruevich, Fiz. Tverd. Tela (Leningrad) **3**, 47 (1961) [Sov. Phys. Solid State **3**, 34 (1961)].
[3] É. A. Kaner and É. P. Fel'dman, Zh. Eksp. Teor. Fiz. **61**, 419 (1971) [Sov. Phys. JETP **34**, 222 (1972)].
[4] I. M. Lifshtz and Kh. I. Pushkarov, Pis'ma Zh. Eksp. Teor. Fiz. **11**, 456 (1970) [JETP Lett. **11**, 310 (1970)].
[5] I. M. Dubrovskiĭ, Ukr. Fiz. Zh. **20**, 1535 (1975).
[6] A. M. Kosevich, Fiz. Nizk. Temp. **4**, 902 (1978) [Sov. J. Low. Temp. Phys. **4**, 429 (1978)].
[7] L. G. Potemina, Fiz. Nizk. Temp. **5**, 261 (1979) [Sov. J. Low Temp. Phys. **5**, 125 (1979)].
[8] J. M. Ziman, Electrons and Phonons, Clarendon Press, Oxford, 1960 (Russ. Transl., IL, M., 1962).
[9] J. Friedel, Dislocations, Pergamon Press, Oxford, 1964 (Russ. Transl. Mir, M., 1967).
[10] M. I. Kaganov, V. Ya. Kravchenko, and V. D. Natsik, Usp. Fiz. Nauk **111**, 655 (1973) [Sov. Phys. Usp. **16**, 878 (1974)].
[11] A. Sugiyama, J. Phys. Soc. Jpn. **21**, 1873 (1966).
[12] L.D. Landau and E. M. Lifshtz, Kvantovaya mekhanika: nerelyativistkaya teoriya, Fizmatgiz, M., 1963 (Quantum Mechanics: Non-Relativistic Theory, 2nd ed., Pergamon Press, Oxford, 1965).
[13] J. D. Eshelby, "Continuum theory of lattice defects," Solid State Phys. **3**, 79 (1956) (Russ. Transl. IL, M., 1963).
[14] M. A. Krivoglaz, Teoriya rasseyaniya rentgenovskikh lucheĭ i teplovykh neitronov real'nymi kristallami, Nauka, M., 1967 (Theory of X-Ray and Thermal Neutron Scattering by Real Crystals, Plenum Press, New York, 1969).
[15] M. B. Partenskiĭ, Fiz. Met. Metalloved. **32**, 510 (1971).
[16] V. D. Natsik and L. G. Potemina, Fiz. Nizk. Temp. **4**, 173 (1978) [Sov. J. Low. Temp. Phys. **4**, 85 (1978)].
[17] V. D. Natsik and L. G. Potemina, Fiz. Nizk. Temp. **5**, 533 (1979) [Sov. J. Low. Temp. Phys. **5**, 258 (1979)].
[18] V. D. Natsik and L. G. Potemina, Fiz. Nizk. Temp. **6**, 620 (1980) [Sov. J. Low. Temp. Phys. **6**, 298 (1980)].

Translated by A. Tybulewicz

High temperature ferromagnetism and the metal–semiconductor transition in an iron chromium sulfide spinel

G. A. Petrakovskiĭ, G. V. Loseva, V. V. Sokolovich, V. P. Ikonnikov, A. V. Baranov, and S. G. Ovchinnikov

Institute of Physics of the Siberian Branch of the USSR Academy of Sciences

(Submitted 30 May 1980)
Zh. Éksp. Teor. Fiz. **79**, 2413–2421 (December 1980)

Results are presented of a comprehensive experimental and theoretical investigation of the metal–semiconductor phase transition in the Fe$_x$Cr$_{1-x}$S system at $x \simeq 0.5$. From an analysis of the structural, electrical, magnetic, thermal, and Mössbauer spectral characteristics it is concluded that the substance obtained, Fe$_2$Cr$_2$S$_4$, which possesses a record-high Curie temperature (940°K) in the semiconducting phase, is in reality the FeCr$_2$S$_4$ spinel with dissolved excess iron atoms. A model of the electronic structure is proposed and explains qualitatively the experimental data. The cause of the metal-semiconductor transition is splitting of the spin subbands upon ferromagnetic ordering.

PACS numbers: 71.30. + h, 75.50.Bb, 72.20.Nz, 71.70. – d

1. INTRODUCTION

The peculiarities of the electronic and crystalline structure of transition-metal sulfides are due to the rich diversity in their electrical and magnetic properties. The main cause of this diversity is the complexity and "mobility" of their electronic structure, which is primarily associated with the lower electronegativity of sulfur compared, for example, with oxygen. In particular, in a number of the indicated compounds a set of distinctive magnetic properties is observed; these are connected with the development of magnetic ordering and the presence of a metal–semiconductor phase transition. Since a basic reorganization of the electronic structure of the material occurs during the metal–semiconductor phase transition, investigation of compounds which combine magnetic ordering with such a transition provide unique opportunities—for example, for detailed study of the role of the electronic subsystem of the material in the development of magnetic ordering. The high-temperature character of the metal–semiconductor phase transition of sulfide compounds compared with vanadium oxides[1] makes the investigation of transition-metal sulfides important with a view toward applications.

Study of the solid solutions $Fe_xCr_{1-x}S$ over a wide range of compositions[2] led to observation at $x = 0.5$ of a spinel structure of nonstoichiometric composition with a record-high Curie temperature $T_C \approx 1000$ °K and a high-temperature metal–semiconductor phase transition. In this paper we present results of a comprehensive investigation of the electric, magnetic, thermal, structural, and Mössbauer characteristics of the nonstoichiometric spinels indicated above. On the basis of this study, we also propose a microscopic model which qualitatively explains the experimental results based on consideration of the electronic energy spectrum.

2. SAMPLES AND EXPERIMENTAL TECHNIQUE

All measurements were carried out on polycrystalline samples which were synthesized in evacuated quartz ampules from 99.99% pure chromium, iron, and sulfur powders in a vertical Silit furnace with programmed control (regulation and maintenance of temperature within 0.1 °C). Batches of chemical reagents of a given composition were heated up to 960 °C in ten hours, held at this temperature for 24 hours, cooled down to 400 °C at a rate of 40 °C per hour, and then the furnace was turned off. The powders obtained were pressed under a pressure of 10 tons/cm² into the form of rectangular rods 5×3×15 mm and were annealed in evacuated quartz ampuls at 1000 °C for three hours.

X-ray analysis of the samples at room temperature was performed on the DRON-1 apparatus (CuK_α radiation with a curved monochromator of the diffractive beam) and the observations during the temperature changes of the crystal lattice were carried out on the URS-50IM apparatus with the GPVT-1500 temperature accessory in a stream of helium.

The differential thermal analysis (DTA) results were obtained on the derivatograph system of F. Paulik, J. Paulik, and L. Erdelyi (Hungary). The derivatograms were taken in specially-shaped sealed and evacuated quartz ampuls up to 1110 °C, with rates of 2.5 and 10 degrees/min on heating and cooling.

Electrical resistance measurements were carried out by the four-probe method in the vacuum chamber of a thermostat in the range 300–1170 °K. Magnetization measurements in the 4.2–300 °K range were carried out in a field of 8 kOe in a pendulum magnetometer, and in the 300–1100 °K range in a field of 0.5 kOe in a ballistic apparatus in quartz evacuated ampuls. The Mössbauer spectra at 300 °K and 77 °K are taken with a Co^{57} source in a chromium matrix.

3. MEASUREMENT RESULTS

The x-ray diffraction measurements at $T = 300$ °K showed that in the $Fe_xCr_{1-x}S$ system, the phase which has the spinel structure $FeCr_2S_4$ is formed in the composition range $0.46 \leq x \leq 0.80$. However, a single-phase composition of the spinel is formed only in a narrow range close to $x = 0.5$. For the remaining compositions, the presence of a second phase in the form of Cr_3S_4, FeS is characteristic. For the composition with $x = 0.5$, besides the lines corresponding to the spinel structure we additionally observed on the diffraction pattern three superstructure lines corresponding to interplanar separations 2.0281, 1.4308, and 1.1750 Å. In the region of these interplanar separations are located both lines from iron and lines from the spinel $FeCr_2S_4$. However, the observed lines do not coincide precisely with either. The unit cell parameter for this sample is $a = 9.994 \pm 0.003$ Å. In the stoichiometric spinel, $a = 9.995 \pm 0.004$ Å. On heating the composition with $x = 0.5$, we observed in the 870 °K region splitting of the (311) lines of the spinel structure on the diffraction pattern. This splitting is retained up to a temperature of 940 °K and disappears on cooling below 670 °K.

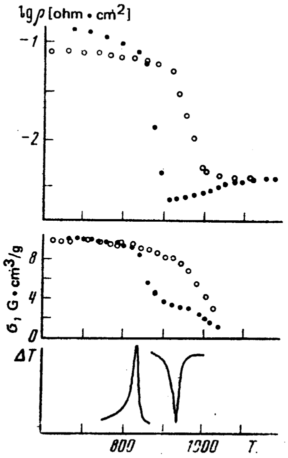

FIG. 1. Temperature dependence of the resistivity (ρ), the magnetization (δ), and the DTA curves in the transition region: ○ heating, ● cooling; DTA endopeaks, heating; DTA exopeaks, cooling.

On Fig. 1 we present the temperature curves for the electrical resistivity ρ and the magnetization σ, along with the DTA curves on heating and cooling. It is obvious that in the 1000 °K region there are two phase transitions: a magnetic transition at the point T_C and a metal–semiconductor phase transition at the temperature T_c, where $T_c < T_C$. The metal–semiconductor phase transition is accompanied by thermal anomalies with appreciable displacement of several lines and the appearance of satellite lines on the diffraction patterns. The latter is evidence for reversible distortion of the spinel lattice. We note that in the stoichiometric spinel $FeCr_2S_4$ we observed a DTA peak at $T = 1300$ °K, which agrees with Ref. 3, where the polymorphous transition $O_h^7 \rightleftarrows D_{6h}^4$ is detected.

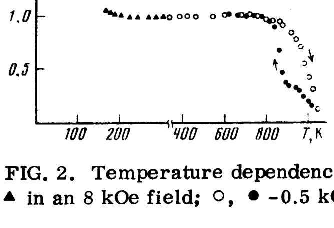

FIG. 2. Temperature dependence of the relative magnetization: ▲ in an 8 kOe field; ○, ● -0.5 kOe.

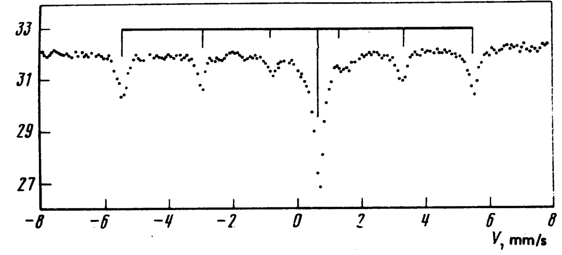

FIG. 3. Mössbauer spectrum at 300°K.

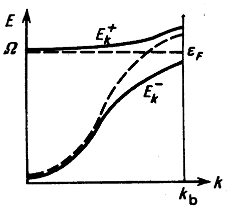

FIG. 4. Electronic structure diagram for the semiconducting stoichiometric spinel $Fe^{2+}Cr_2^{3+}S_4^{2-}$. The dotted line indicates the spectrum without taking hybridization into account.

The temperature dependence of the magnetization for the nonstoichiometric spinel ($x = 0.5$) in the temperature range 4.2–1050 °K is shown on Fig. 2. It is obvious that the shape of the $\sigma(T)$ curves has a complex character and, roughly speaking, may be represented as the superposition of the magnetization of the spinel $FeCr_2S4$ and the weakly temperature-dependent magnetization due to an excess of Fe. The magnetic moment per $Fe_2Cr_2S_4$ formula unit at $T = 300$ °K is equal to 1.91 μ_B, and at 77 °K it is equal to 3.39 μ_B. The Mössbauer spectrum of the nonstoichiometric spinel at 77 °K is a complex pattern of two overlapping sextets. At 300 °K, it is transformed into the superposition of two spectra (Fig. 3). One of them (the singlet) corresponds to the normal spinel $FeCr_2S_4$ (chemical shift $\delta = 0.71 \pm 0.03$ mm/sec) in the paramagnetic phase, in which the Fe^{2+} ions occur in the tetrahedral (A) positions in a strictly cubic environment.[4] The parameters of the second six-component spectrum are close to the parameters of metallic iron ($H_{eff} = 342 \pm 3$ kOe, $\delta = 0.162 \pm 0.01$ mm/sec); however, the quadrupole splitting is different from zero and is equal to $\varepsilon = 0.19 \pm 0.04$ mm/sec. For metallic iron, $H_{eff} = 333 \pm 5$ kOe, $\delta = 0.154 \pm 0.009$ mm/sec, and $\varepsilon = 0$. We note that x-ray diffraction analysis does not detect phases of metallic iron and restricts the possible sizes of the iron particles, if they are present, to ~100 A.

4. DISCUSSION OF RESULTS

The simplest explanation of the high T_c and the magnetization and Mössbauer data parameters is the hypothesis of a two-phase system—i.e., of the existence of macroscopic volumes of metallic iron. However, there is no hysteresis of the magnetization, thermal absorption, and the jump in conductivity of metallic iron. Furthermore, the x-ray diffraction data do not allow us to say if crystalline iron is present. It is possible, finally, that iron exists in an x-ray-amorphous state, but then the large value of T_C and the magnitude of σ are not explained.

We assume that a new chemical compound was formed, in which the excess Fe^{2+} ions are arranged in some orderly fashion (hence the superstructure x-ray diffraction lines) in vacancies of the spinel $FeCr_2S_4$, where there is one Fe^{2+} ion for each "molecule" of $FeCr_2S_4$—i.e., eight ions per cell. Each extra ion gives up two electrons to the unoccupied bands of $FeCr_2S_4$, forming a metallic bond, while the localized states of the Fe^{2+} almost do not form bonds with their neighbors; their electronic configuration d^6 has a localized spin S.

Let us consider in more detail the scheme for the electronic structure of the stoichiometric and enriched spinel. In this case, we proceed from the many-electron model of the similar compounds $CdCr_2S_4$ and $CuCr_2S_4$ which is developed in Refs. 5 and 6. The stoichiometric spinel $Fe^{2+}Cr_2^{3+}S_4^{2-}$ differs from $CdCr_2S_4$ by the absence of four electrons in the molecule; therefore the four holes in the top of the valence band of $CdCr_2S_4$ would have led to metallic properties in $FeCr_2S_4$, since the Fermi level ε_F is located in the band. Therefore to explain the semiconducting properties of the stoichiometric composition $FeCr_2S_4$, we assume that the resonance level $\Omega = E_0(Cr^{3+}) - E_0(Cr^{4+})$, which in $CdCr_2S_4$ lies ~0.2 eV above the top of the valence band,[6] coincides in $Fe^{2+}Cr_2^{3+}S_4^{2-}$ with ε_F. Then hybridization of the band states (which themselves are hybridized states of iron and sulfur) with the chromium states produces a gap at the Fermi level, and the empty upper subband E_k^+ contains four states per molecule (Fig. 4). The spectrum is described by the equation[7]:

$$E_k^{\pm} = {}^1/_2[\varepsilon_k + \Omega \pm ((\varepsilon_k - \Omega)^2 + V^2)^{1/2}], \tag{1}$$

where ε_k is the energy of the band states and V is the hybridization parameter. The gap $E_{min}^+ - E_{max}^-$ in the spectrum may be estimated in terms of the activation energy for $FeCr_2S_4$ and amounts to 0.25–0.30 eV. This scheme qualitatively satisfies the experimentally known facts concerning the characteristics of the electrical conductivity[8] of the stoichiometric or nearly stoichiometric semiconducting spinels $FeCr_2S_4$, according to which both band and atom-like states participate in the transport.

The two extra electrons per molecule make the enriched spinel in the paramagnetic state a metal with a half-filled band (Fig. 5a), the dispersion relation of which $E_{\mathbf{k}}$ may generally speaking differ from $E_{\mathbf{k}}^+$ in Eq. (1). The system of electrons in the $E_{\mathbf{k}}$ band is described by the Hamiltonian

$$H = \sum_{\mathbf{k}\sigma} (E_{\mathbf{k}} - \mu) a_{\mathbf{k}\sigma}{}^+ a_{\mathbf{k}\sigma} + \frac{U}{2} \sum_{\mathbf{f}\sigma} n_{\mathbf{f}}{}^{\sigma} n_{\mathbf{f}}{}^{-\sigma} - J \sum_{\mathbf{f}} \sigma_{\mathbf{f}} S_{\mathbf{f}}. \tag{2}$$

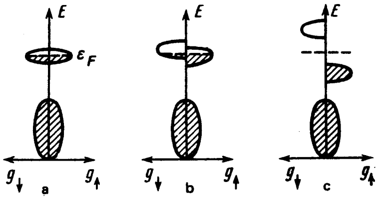

FIG. 5. Diagram of the density of states of the iron-enriched spinel: a) paramagnetic metallic phase; b) ferromagnetic metallic phase; c) ferromagnetic semiconducting phase.

Here the first term describes the band of non-interacting particles with annihilation operators $a_{\mathbf{k}\sigma}$ and chemical potential μ; the second term is the Coulomb interaction of the band electrons, where within the spirit of the Hubbard model only the intra-atomic Coulomb matrix element U remains (the point being that the band $E_{\mathbf{k}}$ is narrow due to the high charge density at the top of the original band $\varepsilon_{\mathbf{k}}$, determined by the large contribution of the iron states). Here $n_{\mathbf{f}}^{\sigma}=a_{\mathbf{f}\sigma}^{+}a_{\mathbf{f}\sigma}$, the index f numbers the lattice points, and

$$a_{\mathbf{f}\sigma}=N^{-1/2}\sum_{\mathbf{k}}a_{\mathbf{k}\sigma}\exp(i\mathbf{kf}).$$

The third term in Eq. (2) describes the $s-d$ exchange interaction of the localized spin S of the extra Fe^{2+} ion with the spin σ of the band electrons. This interaction is short-range; therefore in Eq. (2) only terms at the single lattice point remain. Generally speaking, there may be an $s-d$ exchange interaction also with the localized spins of the Cr^{3+} and Fe^{2+} ions belonging to the $FeCr_2S_4$ matrix; however, we assume that the band electrons are spatially sufficiently localized close to the extra Fe^{2+} ions and, due to the short range of the $s-d$ exchange integral, such interaction is negligibly small. For simplicity, instead of a four-band scheme with two electrons, we consider a nondegenerate two-band scheme with a single electron, $n=1$. In the simplest mean-field approximation we find the one-electron Green's function

$$G_{\sigma}(\mathbf{k},E)=(E-E_{\sigma}(\mathbf{k}))^{-1},\quad E_{\sigma}(\mathbf{k})=E_{\mathbf{k}}+\delta\mu-\eta(\sigma)\Delta;$$
$$\eta(\sigma)=+1,\ \sigma=\uparrow;\quad \eta(\sigma)=-1,\ \sigma=\downarrow. \tag{3}$$

Here $\delta\mu=Un/2-\mu$, $\Delta=U\langle\sigma^{z}\rangle+J\langle S^{z}\rangle/2$ is the analog of the Stoner gap in the band theory of magnetism, but enhanced due to the interaction with the localized spins. The chemical potential μ, the band moment $\langle\sigma\rangle$, and the localized moment $\langle S\rangle$ should be determined in a self-consistent manner.

The self-consistency equation for

$$n=N^{-1}\sum_{\mathbf{k}\sigma}\langle a_{\mathbf{k}\sigma}{}^{+}a_{\mathbf{k}\sigma}\rangle$$

may be represented as

$$1-n=\frac{1}{2}\int_{-W}^{W}g(\varepsilon)d\varepsilon\left[\operatorname{th}\frac{\varepsilon+\delta\mu-\Delta}{2T}+\operatorname{th}\frac{\varepsilon+\delta\mu+\Delta}{2T}\right]. \tag{4}$$

Here $g(\varepsilon)$ is the density of states of the band $E_{\mathbf{k}}$, the half-width of which is W, and the reference for the energy is the center of the band. From Eq. (4) it is obvious that at $n=1$, $\delta\mu=0$ for all temperatures [if $g(\varepsilon)$ is an even function of ε].

The equation for the band magnetization is

$$\langle\sigma\rangle=\frac{1}{2N}\sum_{\mathbf{k}}(\langle a_{\mathbf{k}\uparrow}{}^{+}a_{\mathbf{k}\uparrow}\rangle-\langle a_{\mathbf{k}\downarrow}{}^{+}a_{\mathbf{k}\downarrow}\rangle)$$
$$=\frac{1}{2}\int_{0}^{W}g(\varepsilon)d\varepsilon\left[\operatorname{th}\frac{\varepsilon+\Delta}{2T}-\operatorname{th}\frac{\varepsilon-\Delta}{2T}\right]. \tag{5}$$

In the mean-field approximation, an effective field

$$\mathscr{H}_{\text{eff}}=-J\langle\sigma\rangle\sum_{\mathbf{f}}S_{\mathbf{f}}{}^{z},$$

acts at each spin; therefore

$$\langle S\rangle=\operatorname{Sp}(S_{\mathbf{f}}{}^{z}e^{-H/T})/\operatorname{Sp}(e^{-H/T})=SB_{S}(J\langle\sigma\rangle/T), \tag{6}$$

where $B_S(x)=(1+\frac{1}{2}S)\coth(1+\frac{1}{2}S)x-\frac{1}{2}S\coth x/2S$ is the Brillouin function for the spin S.

Equations (5) and (6) form a system of equations for $\langle\sigma\rangle$ and $\langle S\rangle$, the solution of which also allows us to find the gap Δ. Let us consider first the solution of this system for $T=0$. In this case

$$\langle S\rangle=S\operatorname{sign}(J). \tag{7}$$

The factor sign (J) reflects the fact that for $J>0$ the localized spins are parallel to the band spins, and for $J<0$ they are antiparallel. Due to this factor, the gap Δ does not depend on the sign of J, $\Delta=U\langle\sigma\rangle+|J|S/2$. From Eq. (5) for $T=0$ it follows that

$$\langle\sigma\rangle=\int_{0}^{\Delta}g(\varepsilon)d\varepsilon=N(\Delta)-{}^{1}/{}_{2}\leqslant{}^{1}/{}_{2}, \tag{8}$$

where $N(E)$ is the number of states with energies not exceeding E,

$$N(E)=\int_{-W}^{E}g(\varepsilon)d\varepsilon.$$

In particular, in the rectangular band model $g(\varepsilon)=W/2$ it follows from Eq. (8) that $\sigma=\Delta/2W$. The final form of the self-consistency equation at $T=0$ for $\langle\sigma\rangle$ is the following:

$$\langle\sigma\rangle=\lambda_{c}\langle\sigma\rangle+\lambda_{cd}S/2, \tag{9}$$

where the dimensionless interaction parameters $\lambda_c=U/2W$ and $\lambda_{cd}=|J|/2W$ are introduced. We note that for $J=0$ we obtain from Eq. (9) the well-known Stoner criterion for the existence of band ferromagnetism (see, for example, Ref. 9):

$$\lambda_{c}>1. \tag{10}$$

In our case, the solution to Eq. (9) is

$$\langle\sigma\rangle=\lambda_{cd}S/2(1-\lambda_{c}). \tag{11}$$

We note that the theory is applicable for λ_c, $\lambda_{cd}\ll 1$; therefore the formal divergence of Eq. (11) as $\lambda_c\to 1$ does not have a physical meaning. If λ_c or $|J|S$ are so large that $\Delta>W$, then the equality holds in Eq. (8); so that the maximum value of $\langle\sigma\rangle$ is equal to 1/2, as it should be.

As $T\to T_C$ we have $\langle\sigma\rangle$, $\langle S\rangle\to 0$; and for the Curie temperature we have the equation

$$T_{C}=\frac{1}{2}\left(U+\frac{J^{2}(S+1)}{6T_{C}}\right)\int_{0}^{W}g(\varepsilon)d\varepsilon\operatorname{ch}^{-2}\left(\frac{\varepsilon}{2T_{C}}\right). \tag{12}$$

In the rectangular band model the solution of Eq. (12) in the region $T_C\ll W$ is

$$T_{C}=W\frac{S+1}{3}\frac{\lambda_{cd}{}^{2}}{1-\lambda_{c}}. \tag{13}$$

From Eqs. (11) and (13) it is obvious that the Coulomb interaction strengthens the exchange magnetization of the band electrons, as is usual for the $s-d$ model, and increases the Curie temperature compared with the value $T_C^{(0)}\sim W\lambda_{cd}^2$, as is usual for the $s-d$ model.

In the ferromagnetic phase, the spin subbands are separated by the gap Δ, and close to T_C when $\Delta<W$, the bands overlap (Fig. 5b) and the material is a ferromagnetic metal. On further lowering of T, the magnet-

ization and Δ increase; and when the condition $\Delta \geqslant W$ is satisfied for $T \leqslant T_c \leqslant T_C$, the spin subbands are separated by the gap $E_g = \Delta - W$ (Fig. 5c). Since the original band was half-filled, the lower subband is filled completely (at $T = 0$); i.e., for $T < T_c$ we have a ferromagnetic semiconductor with a magnetic moment per molecule of

$$\sigma = 2(2\langle\sigma\rangle + \langle S\rangle)\mu_B. \tag{14}$$

Here the factor 2 before the $\langle\sigma\rangle$ reflects the fact that there were two electrons in the conduction band of the metallic phase. The magnitude of the localized spin S depends on where the extra Fe^{2+} ion falls—in an A position or a B position—and also on whether the high-spin or low-spin state of the ion is the ground state (i.e., on the relationship between the intra-atomic Coulomb interaction and the crystal field). The possible states for the d^6 configuration will be: in the A-position (tetrahedral environment):

1) orbital doublet, $S = 2$—high-spin state;

2) orbital triplet, $S = 1$—low-spin state;

in the B-position (octahedral environment):

3) orbital triplet, $S = 2$—high-spin state;

4) orbital singlet, $S = 0$—low-spin state.

Since in the semiconductor phase $\langle\sigma\rangle = \frac{1}{2}$ for $T = 0$, agreement with the experimental values of $\sigma \approx 2\mu_B$ is impossible for case 2; for cases 1 and 3 it is possible only for $J < 0$. In this case, the localized spins are oriented opposite to the band spins. In case 4, the magnetic properties are due only to the band electrons. Since the orbital degeneracy is different in all three possible situations, they may be distinguished experimentally.

The ions of the matrix Cr^{3+} and Fe^{2+} apparently will be in a paramagnetic state for $T_N < T < T_c$, where T_N is determined by the interaction with the matrix itself. This circumstance follows from the short range of the intra-atomic $s-d$ exchange interaction, and for the Fe^{2+} ion is confirmed by Mössbauer data. On these grounds, the magnetic moment (Eq. 14) and the Curie temperature are close to the corresponding parameters for metallic iron. The difference in electrical properties (the lack of a metal-dielectric transition in metallic iron) is connected with the fact that in iron the narrow d-band overlaps with the broad s-band and the condition $\Delta > W$ is not satisfied. In our case, there is only one narrow d-band, $2W \sim 1$ eV, and the gap Δ has a magnitude close to the value for iron[10] $2\Delta = 1-1.5$ eV. Therefore the condition $\Delta > W$ may be realized. Our experimental value $E_g = 0.25-0.3$ eV is consistent with the estimates given above for W and Δ. When, as T increases, the magnetization and $\Delta(T)$ are decreased so that $E_g(T) \leqslant 0$, we go over to a metallic ferromagnetic phase at the temperature T_c. In the simple model with the Hamiltonian in Eq. (2), this transition in the mean-field approximation is a second-order transition. To obtain a first-order transition, it is necessary to take into account the connection of the magnetic and elastic subsystems.[7] Then we may obtain a jump in magnetic moment at the point $T_c < T_C$, and in this case the jump in Δ to the value Δ $\Delta < W$. This connection also explains the distortion of the lattice in the vicinity of T_c.

Since in Co^{2+} and Ni^{2+} the localized moments are less, Δ_{Co}, $\Delta_{Ni} < \Delta_{Fe}$ (for Ni, $\Delta = 0.15-0.20$ eV)[10], therefore on going to the spinels with Co and Ni the metallic properties are enhanced. Thus, in Ni-enriched $NiCr_2S_4$, the condition $\Delta > W$ generally is not satisfied and this compound is metallic at all temperatures, which agrees with our preliminary results.

Since the excess Fe^{2+} ion occurs in a state close to the state of the ions in metallic Fe (according to the magnitude of the magnetic moment, the number of electrons per cation), the similarity of the Mössbauer spectra of our sample and that of Fe is understandable. The appearance of a quadrupole splitting is a consequence of the change in symmetry of the environment.

Our data does not so far allow us to say unambiguously in which lattice vacancies of the spinel the extra Fe^{2+} ion falls.

5. CONCLUSION

Thus, our investigation showed that in the system of $Fe_xCr_{1-x}S$ solid solutions with $x \approx 0.5$, nonstoichiometric semiconducting spinel phase is formed which is characterized by a record-high Curie temperature and by the presence of a metal–semiconductor phase transition. Analysis of the structural, electrical, magnetic, thermal, and Mössbauer studies allow us to assume that the material obtained ($Fe_2Cr_2S_4$) is the spinel $FeCr_2S_4$ with excess iron atoms dissolved in it.

The proposed model of the electronic structure of the stoichiometric and the iron-enriched spinels $FeCr_2S_4$ qualitatively explains the available experimental data. Furthermore, it predicts that ferromagnetic ordering of the excess iron and the absence of ordering of the chromium ions is more probable than ferromagnetic ordering with formation of a chromium sublattice (for $T > 180$ °K).

[1] A. A. Bugaev, B. P. Zakharchenya, and F. A. Chudnovskiĭ, Fazovy perekhod metall—poluprovodnik i ego primenenie (The Metal—Semiconductor Phase Transition and Its Applications), Nauka, 1979.

[2] G. V. Loseva, S. G. Ovchinnikov, V. V. Sokolovich, and E. P. Petukhov, Fiz. Tverd. Tela (Leningrad) 19, 2922 (1977) [Sov. Phys. Solid State 19, 1713 (1977)].

[3] R. J. Bouchard, Mat. Res. Bull. 2, 459 (1967).

[4] L. M. Belyaeva, G. V. Dmitrieva, I. S. Lyubutin, A. P. Mazhara, and V. V. Fedorov, Zh. Éksp. Teor. Fiz. 68, 1176 (1979) [Sov. Phys. JETP 41, 583 (1975)].

[5] M. Sh. Erukhimov and S. G. Ovchinnikov, Fiz. Tverd. Tela (Leningrad) 21, 351 (1979) [Sov. Phys. Solid State 21, 209 (1979)].

[6] S. G. Ovchinnikov, Fiz. Tverd. Tela (Leningrad) 21, 2994 (1979) [Sov. Phys. Solid State 21, 1724 (1979)].

[7] E. V. Kuz'min, G. A. Petrakovskiĭ, and É. A. Zavadskiĭ, Fizika magnitouporyadochennykh veshchestv (Physics of Magnetically Ordered Materials), Nauka, 1976.

[8] T. Watanabe, Solid State Commun. 12, 355 (1973).

[9] S. V. Vonsovskiĭ, Magnetizm. Magnitnye svoĭstva dia-, para-, ferro-, antiferro-, i ferrimagnetikov, (Magnetism. Magnetic Properties of Dia-, Para-, Ferro-, Antiferro-, and Ferrimagnets), Nauka, Moscow, 1971. 1032 pp.

[10] E. I. Kondorskiĭ, Zonnaya teoriya magnetizma (Band Theory of Magnetism), Part 1, Izdat. MGU, 1976.

Translated by Cathy Flick